Corrosion Science xxx (2010) xxx–xxx

Contents lists available at ScienceDirect

Corrosion Science

journal homepage: www.elsevier.com/locate/corsci

On the substitution of conventional corrosion tests by an electrochemical potentiokinetic reactivation test

M. Prohaska [a,*], H. Kanduth [a], G. Mori [a], R. Grill [a], G. Tischler [b]

[a] CD-Laboratory of Localized Corrosion, University of Leoben, Franz-Josef-Straße 18, 8700 Leoben, Austria
[b] Voestalpine Grobblech GmbH, Voest-Alpine-Straße 3, 4031 Linz, Austria

ARTICLE INFO

Article history:
Received 16 January 2009
Accepted 17 January 2010
Available online xxxx

Keywords:
A. Alloy 625
B. Polarization
C. Intergranular corrosion

ABSTRACT

Nickel-based alloy 625 was investigated by means of a conventional corrosion test (Streicher-test according to ASTM G28A [1]) and an electrochemical potentiokinetic reactivation test (according to ASTM G108 [1], with some modifications). Susceptibility to intergranular corrosion after various heat treatments was examined by using both test methods and the results were compared. Dependent on the type of heat treatment applied, both methods showed partially different results. Possibilities and limitations of replacing Streicher-test with EPR-test are pointed out and commentated. In conclusion, the EPR-test presents itself as a promising and quick investigation technique for detecting susceptibility to intergranular corrosion in nickel-based alloys.

1. Introduction

The electrochemical potentiokinetic reactivation test (EPR) is a quasi non-destructive test to describe the corrosion resistance of steels and nickel-based alloys. The EPR-method was developed by Cihal et al. [2] in 1969 with further improvements being made in the following decades [3]. This test is employed primarily to determine the degree of sensitization (DOS), i.e. the materials susceptibility to IGA, but can also provide information on the general corrosion resistance and how this is affected by microstructural changes [4,5]. Compared to conventional corrosion tests, the EPR-test exhibits a couple of advantages: It is much quicker, more sensitive and more accurate, particularly for highly sensitized specimens. In general, two different types of the EPR-test were developed over the years, the double loop [6–8] and the single loop [8–10] test. In the single loop EPR-test the polarization curve is a reverse curve, with a potential scan from the passive range to open circuit potential (OCP). In contrast, the double loop EPR-test shows a cyclic polarization curve consisting of a forward scan followed by a reverse scan starting at active OCP. In this case a holding time at a certain vertex potential (usually located in the passive or the transpassive region) is possible. For stainless steels 304 and 304 L the EPR-test parameters are prescribed in ASTM G108 [1].

The main focus of this work was the investigation of the susceptibility to intergranular corrosion of the nickel-based alloy 625 after different heat treatments, sensitization times and sensitization temperatures, by means of the double loop EPR-test.

Alloy 625 is a wrought nickel-based superalloy strengthened mainly by the addition of carbon, chromium, molybdenum and niobium [11]. Two different types of alloy 625 are available on the market: a low carbon type (less than 0.026% carbon) for wet corrosion applications (normally used in stabilization annealed condition) and a high carbon type (about 0,045% carbon) for high temperature applications (normally used in solution annealed condition). Typically stabilization annealing is performed in a temperature range of 940–980 °C and yields predominantly to primary NbC precipitation and to secondary carbide precipitation of M_6C and NbC. Solution annealing is usually carried out at temperatures between 1100 and 1150 °C, so solution annealed specimens may contain primary NbC. Alloy 625 combines the high strength of age-hardened nickel-based alloys with good fabrication characteristics. Furthermore, alloy 625 is used as a cladding material for corrosion resistant pipes for oil and gas industry [12]. The fabrication of these pipes is conducted by means of a thermo-mechanical rolling process, which on the one hand improves the mechanical properties of the base material and on the other hand leads to sensitization of the cladding material between 600 and 950 °C. During this sensitization process precipitation hardening takes place in the cladding material. This is mainly due to the precipitation of the metastable η''-phase Ni_3(Nb,Mo,Al,Ti) [13]. It is known that precipitation of $\delta - Ni_3Nb$ phase leads to sensitization of alloy 625 in oxidizing media [14]. Furthermore precipitation of $M_{23}C_6$ and M_6C [15] carbides occurs in a temperature range of 660–1050 °C, precipitation of MC takes place above 1050 °C. Fig. 1 gives an overview of precipitation characteristics, especially those of carbides, in alloy 625 investigated by different authors [16–19]. All mentionable precipitates nucleate preferably on grain boundaries

* Corresponding author. Tel.: +43 3842 402 1220; fax: +43 3842 402 1252.
E-mail address: manuel.prohaska@unileoben.ac.at (M. Prohaska).

0010-938X/$ - see front matter © 2010 Elsevier Ltd. All rights reserved.
doi:10.1016/j.corsci.2010.01.017

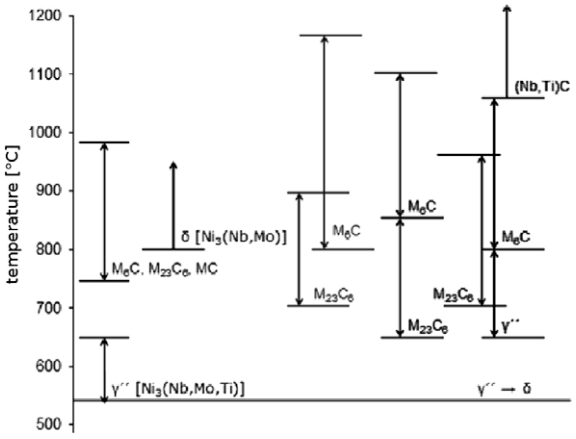

Fig. 1. Temperature range of carbide and η''-phase precipitation in alloy 625 (solution annealed condition) [16–19].

and may lead to (dependent on their chemical composition) a depletion of mainly chromium and/or molybdenum adjacent to the grain boundaries. Hence corrosion resistance in these zones is dramatically reduced and the susceptibility to intergranular corrosion is strongly enhanced.

The results described in this paper were determined by means of EPR-test (based on ASTM G108) and a ferric-sulfate–sulfuric-acid immersion test (Streicher-test) according to ASTM G28A. The results of both investigation techniques were compared and evaluated.

2. Experimental method

2.1. Chemical composition and heat treatment parameters

The current investigation was conducted on aged plate material of alloy 625. Its chemical composition is shown in Table 1 in detail.

After hot rolling to plates of 8 mm thickness the samples were subjected either to solution annealing at 1120 °C for 4 h or to stabilization annealing at 960 °C for 3 h followed by water quenching. Subsequently the plates were cut and additional heat treatments were performed by using electric furnaces under ambient air. The specific heat treatment parameters are shown in Fig. 2 and Table 2. After annealing samples with a size of $40 \times 20 \times 8$ mm^3 (for Streicher-test) and $10 \times 10 \times 8$ mm^3 (for the EPR-test) were cut from the plates. Reference material was the stabilization annealed condition (A) on the one hand and the solution annealed condition (B), on the other hand.

2.2. Test solution

One litre of the used EPR-test solution was composed of 146 ml sulfuric acid (H_2SO_4), 238 ml hydrochloric acid (HCl) and 0.001 M potassium thiocyanate (KSCN) as an activator mixed with laboratory-grade distilled water.

Streicher-test solution was composed of 236 ml sulfuric acid (H_2SO_4), 25 g iron (III) sulfate hydrate ($Fe_2(SO_4)_3$. xH_2O) and 400 ml distilled water.

2.3. Test procedure

All samples (for Streicher-test as well as for EPR-test) were surface-finished using final 4000-grit abrasive SiC-paper. The Streicher-test was performed at a temperature of boiling sulfuric acid for a time of 120 h. This test procedure was according to ASTM G28A.

The test procedure of the EPR-test based on ASTM G108, with some modifications: It had to be assured, that all samples were in an active condition. Regarding this fact, the measurement had to be started within a maximum time of 3 min after surface finishing and cleaning with acetone to avoid the formation of a overly thick protective oxide layer. After the solution was poured into the electrochemical cell, a delay of 40 min was maintained to assure homogenous temperature of the test solution. Particular

Table 1
Chemical composition of alloy 625 according to Thyssen Krupp VDM (in wt.%).

Material number	Ni (wt.%)	Cr (wt.%)	Mo (wt.%)	Fe (wt.%)	Co (wt.%)	W (wt.%)	Mn (wt.%)	Si (wt.%)	Ti (wt.%)	Nb (wt.%)	C (wt.%)
2.4856	61.09	22.10	9.10	3.50	0.10	0.15	0.04	0.14	0.20	3.42	0.026

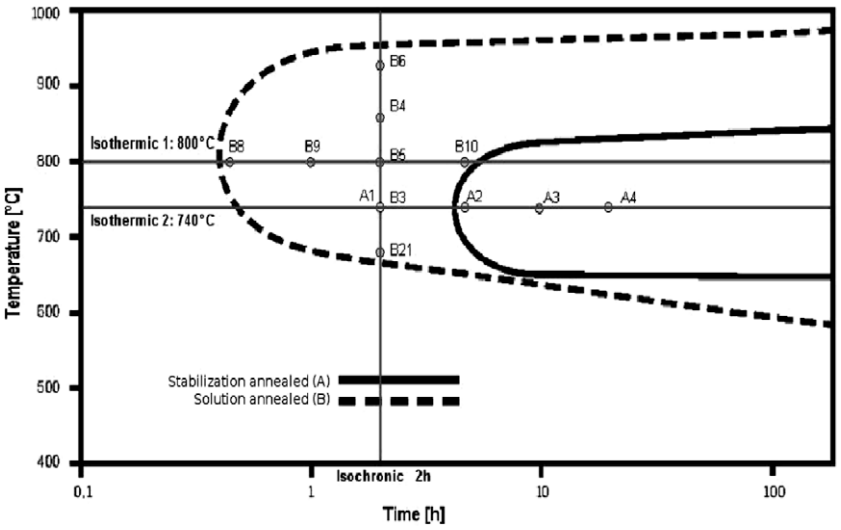

Fig. 2. Heat treatments conducted on alloy 625.

Please cite this article in press as: M. Prohaska et al., On the substitution of conventional corrosion tests by an electrochemical potentiokinetic reactivation test, Corros. Sci. (2010), doi:10.1016/j.corsci.2010.01.017

Table 2
Heat treatment data.

Heat treatment description	Annealing condition	Sensitization temperature (°C)	Sensitization time (h)
A	Stabilization annealed	–	–
A1	Stabilization annealed	740	2
A2	Stabilization annealed	740	5
A3	Stabilization annealed	740	10
A4	Stabilization annealed	740	20
B	Solution annealed	–	–
B21	Solution annealed	680	2
B3	Solution annealed	740	2
B5	Solution annealed	800	2
B4	Solution annealed	860	2
B6	Solution annealed	920	2
B7	Solution annealed	980	2
B8	Solution annealed	800	0.5
B9	Solution annealed	800	1
B10	Solution annealed	800	5

Table 3
Test parameters.

	Scan rate (mV/s)	Vertex potential (mV)	Solution temperature (°C)	Activator concentration (mol/l)
standard	1.67	+200	30	0.001

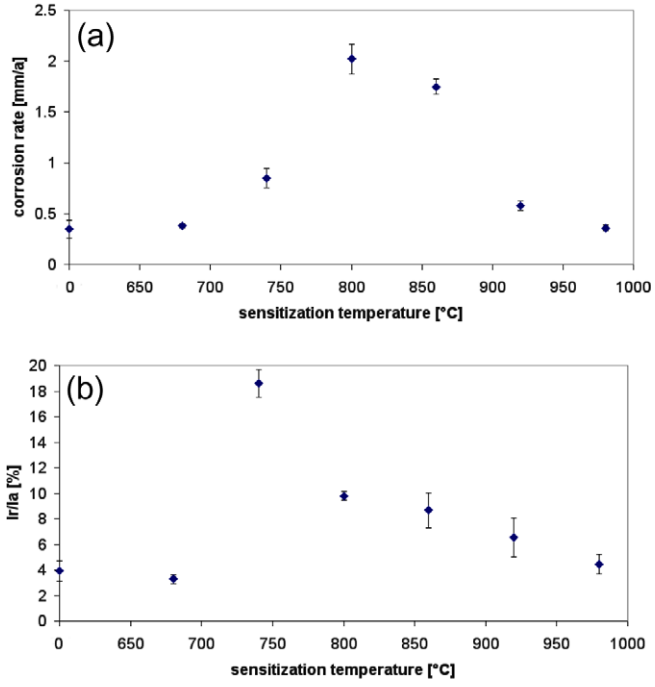

Fig. 3. Corrosion rate of Streicher-test (a) and Ir/Ia values of EPR-test (b) as function of sensitization temperature - solution annealed condition + sensitization for 2 h.

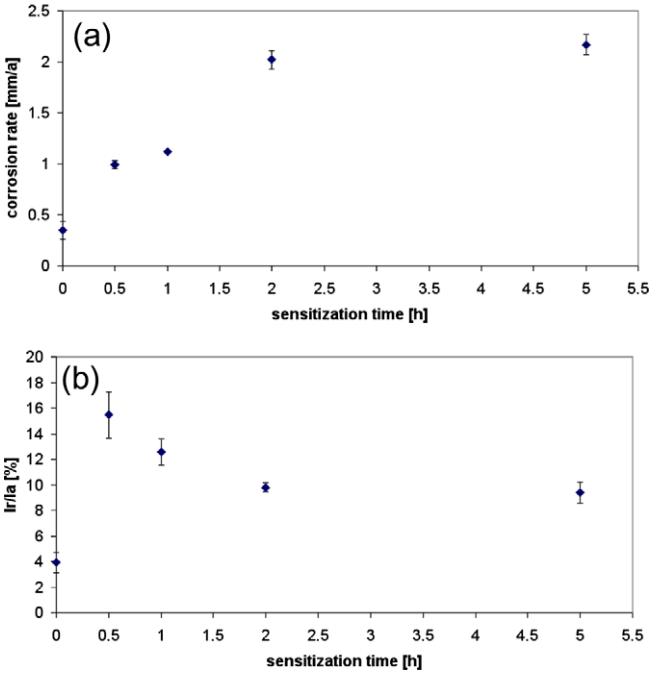

Fig. 4. Corrosion rate of Streicher-test (a) and Ir/Ia values of EPR-test (b) as function of sensitization time – solution annealed condition + sensitization at 800 °C.

attention was paid to the pH-value of the reference electrode solution (saturated potassiumchloride) as it influences the results dramatically. Reduction of the pH-value may occur by acidification of the reference electrode solution caused by the very acidic test solution. Argon was used to stir the solution during the experiment to ensure an oxygen free electrolyte. The open circuit potential (OCP) was measured for 2 min and there was no delay at the vertex potential. The current density ratio (Ir/Ia) was calculated and evaluated.

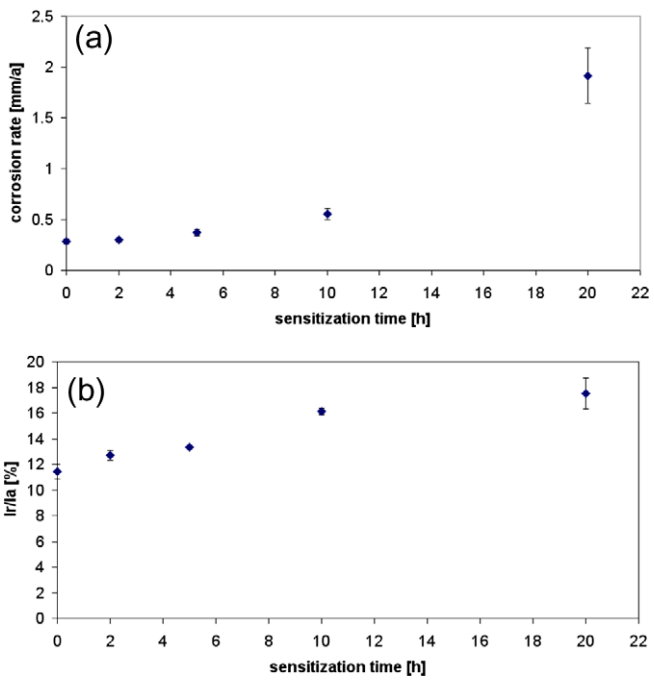

Fig. 5. Corrosion rate of Streicher-test (a) and Ir/Ia values of EPR-test (b) as function of sensitization time – stabilization annealed condition + sensitization at 740 °C.

Please cite this article in press as: M. Prohaska et al., On the substitution of conventional corrosion tests by an electrochemical potentiokinetic reactivation test, Corros. Sci. (2010), doi:10.1016/j.corsci.2010.01.017

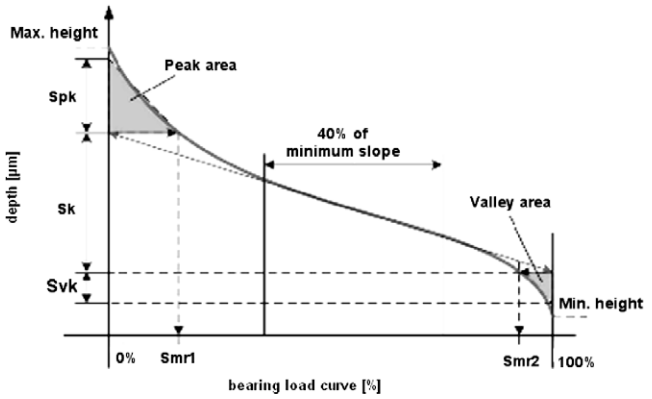

Fig. 6. Surface parameters according to Alicona Software IFM 2.2 – area analysis [21].

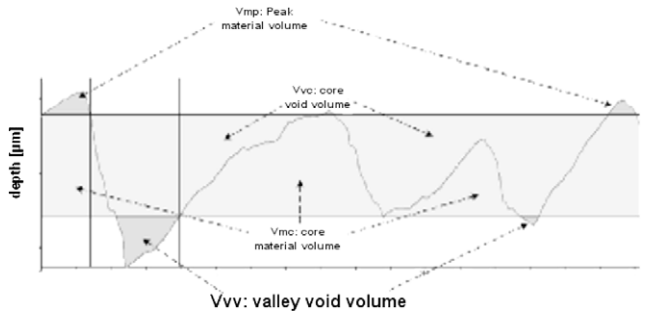

Fig. 7. Volume parameters according to Alicona Software IFM 2.2 – area analysis [21].

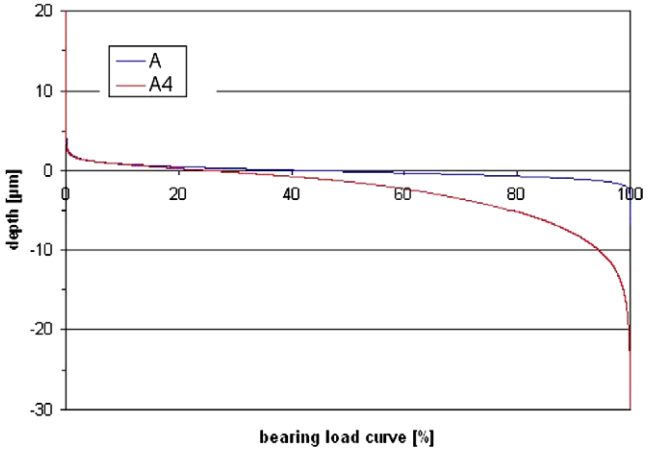

Fig. 8. Bearing load curve of non-sensitized and sensitized stabilization annealed alloy 625.

The effect of the performed heat treatments on susceptibility to intergranular corrosion was investigated by means of EPR- and Streicher-tests. The chosen test parameters for the EPR-tests are shown in Table 3 and have been optimized in earlier research [20].

All tested samples were additionally analysed by scanning electron microscopy. The microscope used for the current investigations was a Zeiss Instruments, type "Evo 50".

3. Results

3.1. Comparison of Streicher-test and EPR-test

3.1.1. Solution annealed specimens + sensitization for 2 h at various temperatures

Fig. 3 shows the results of solution annealed and sensitized specimens for the Streicher-test (Fig. 3a) and for EPR-test (Fig. 3b).

The highest corrosion rate measured in the Streicher-test occurred after sensitization at 800 °C (Fig. 3a). The corrosion rate sharply increased at approximately 680 °C, reached a maximum at 800 °C and thereafter declined. The results of the EPR-test were similar to those obtained of the Streicher-test, but highest Ir/Ia-ratio was seen at a sensitization temperature of 740 °C instead of 800 °C (Fig. 3b). The Ir/Ia-ratio of 740 °C was approximately twice the value of the current density ratio at 800 °C.

3.1.2. Solution annealed specimens + sensitization at 800 °C for various times

Fig. 4 shows the results of Streicher-test (Fig. 4a) as well as those of EPR-test (Fig. 4b).

The corrosion rate of the material investigated increased with increasing sensitization time for the Streicher-test. The EPR-test showed the highest Ir/Ia-ratio after 0.5 h of sensitization at 800 °C, but after longer sensitization times the current density ratio declined.

3.1.3. Stabilization annealed specimens + sensitization at 740 °C for various times

Fig. 5 shows the results of Streicher-test (Fig. 5a) and those of EPR-test (Fig. 5b).

The corrosion rate of stabilization annealed samples only slightly increased during the Streicher-test up to a time of 10 h whereas after 10 h of sensitization a sharp increase was observed (Fig. 5a). Additionally, the standard deviation of the performed Streicher-tests continuously increased with longer sensitization times. The Ir/Ia-ratios determined in the EPR-test initially showed similar dependency on sensitization time as the Streicher-tests, but no such striking increase was seen after 10 h of sensitization. Indeed there was almost no further increase in the Ir/Ia-ratios after 20 h of sensitization (Figs. 5a and 5b).

Table 4
Sample surface characterisation after Streicher-tests.

Heat treatment discription	Sensitization temperature (°C)	Sensitization time (h)	Valley void volume (Vvv) (ml/m^2)	Reduced valley height (Svk) (µm)
A	–	–	0.09 ± 0.004	0.86 ± 0.04
A3	740	10	0.25 ± 0.01	2.53 ± 0.02
A4	740	20	0.75 ± 0.02	7.74 ± 0.11
B	–	–	0.27 ± 0.08	2.71 ± 0.86
B3	740	2	0.93 ± 0.06	9.34 ± 0.30
B5	800	2	1.83 ± 0.36	18.76 ± 3.47
B4	860	2	0.47 ± 0.08	5.02 ± 0.63
B	–	–	0.27 ± 0.08	2.71 ± 0.86
B8	800	0.5	0.84 ± 0.28	8.83 ± 1.23
B10	800	5	1.94 ± 0.36	19.53 ± 2.93

Please cite this article in press as: M. Prohaska et al., On the substitution of conventional corrosion tests by an electrochemical potentiokinetic reactivation test, Corros. Sci. (2010), doi:10.1016/j.corsci.2010.01.017

3.2. Three-dimensional Optical Microscopy

In order to quantificate the extent of dissolved material during Streicher-tests, investigations by means of a three-dimensional optical microscope (type Alicona imaging Infinite Focus G3) were performed. The examined surface area was rectangular with a size of $2.5 \times 3.5\ mm^2$. Analysis was done by using the area analysis function of software IFM 2.2. Relevant surface parameters (on the basis of IFM 2.2 area analysis – Vvv and Svk) for sample characterisation were evaluated for most sensitized as well as for non-sensitized specimens. Vvc is contributed to the amount of dropped grains, whereas the parameter Svk describes the average depth of surface voids caused by grain dropping. A detailed explanation of the evaluated surface and volume parameters is presented in Figs. 6 and 7.

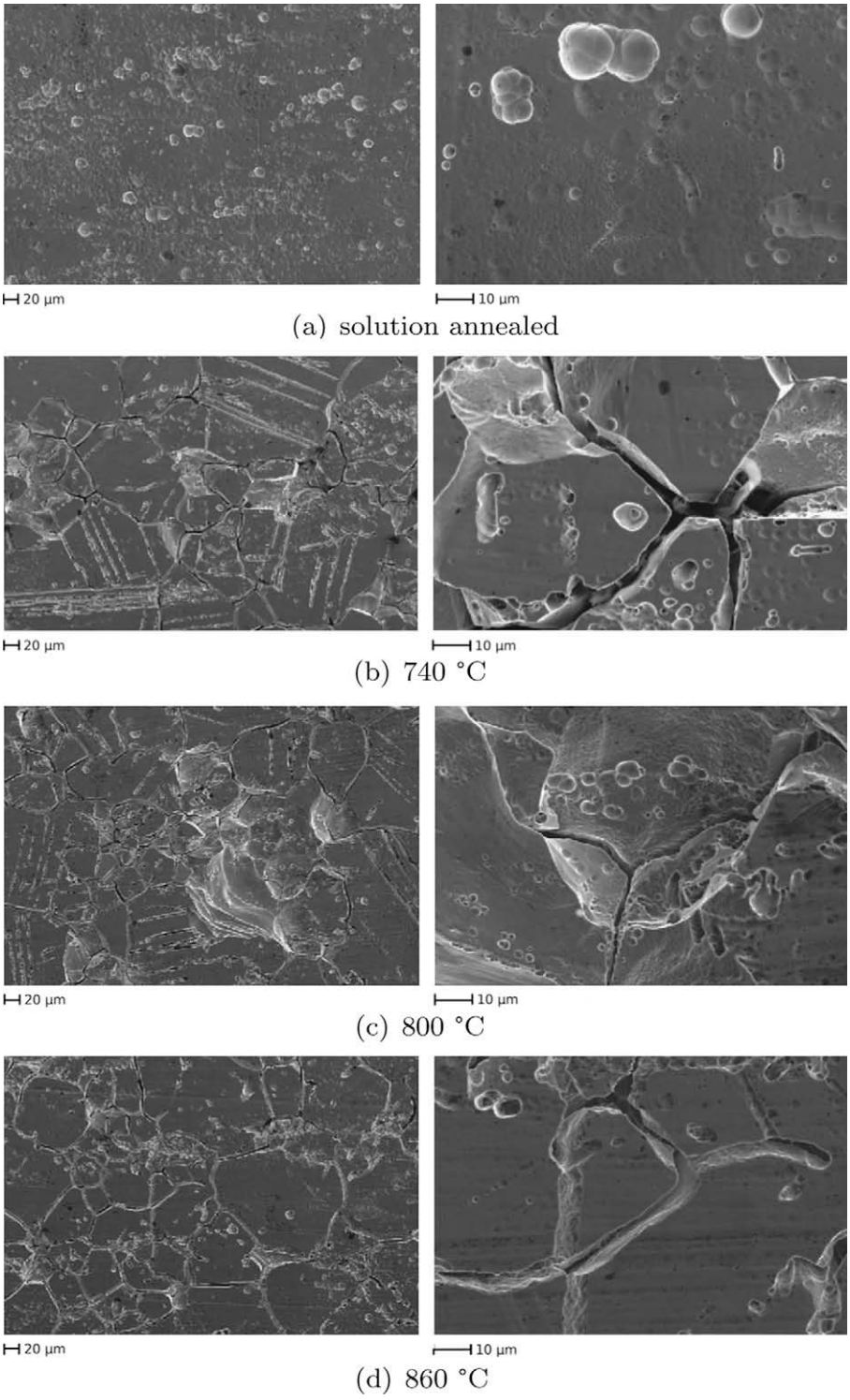

Fig. 9. Microstructural characterisation of Streicher-test by means of SEM – solution annealed specimens + sensitization for 2 h at variable temperatures. (a) Solution annealed (b) 740 °C (c) 800 °C (d) 860 °C.

Please cite this article in press as: M. Prohaska et al., On the substitution of conventional corrosion tests by an electrochemical potentiokinetic reactivation test, Corros. Sci. (2010), doi:10.1016/j.corsci.2010.01.017

Fig. 8 shows measured bearing load curves of sensitized and non-sensitized alloy 625. The valley void volume as well as the reduced valley height is higher after 20 h of sensitization.

The quantitative results of all investigated samples are shown in Table 4. Each heat treatment condition was measured three times.

3.2.1. Solution annealed specimens + sensitization for 2 h at various temperatures

The dissolved volume as well as the depth of the attack is clearly highest after sensitization at 800 °C. This is in confirmation with Fig. 3 whereas the highest corrosion rate was evaluated after sensitization at 800 °C. The second-highest amount of dissolved volume was obtained after sensitization at 740 °C, whereas the third-highest amount of dissolved volume was evaluated after sensitization at 860 °C. The average depth of attack shows the same dependency.

3.2.2. Solution annealed specimens + sensitization at 800 °C for various times

Depth of attack as well as dissolved volume is clearly higher after 5 h of sensitization time compared to 0.5 h. These results are consistent with Fig. 4.

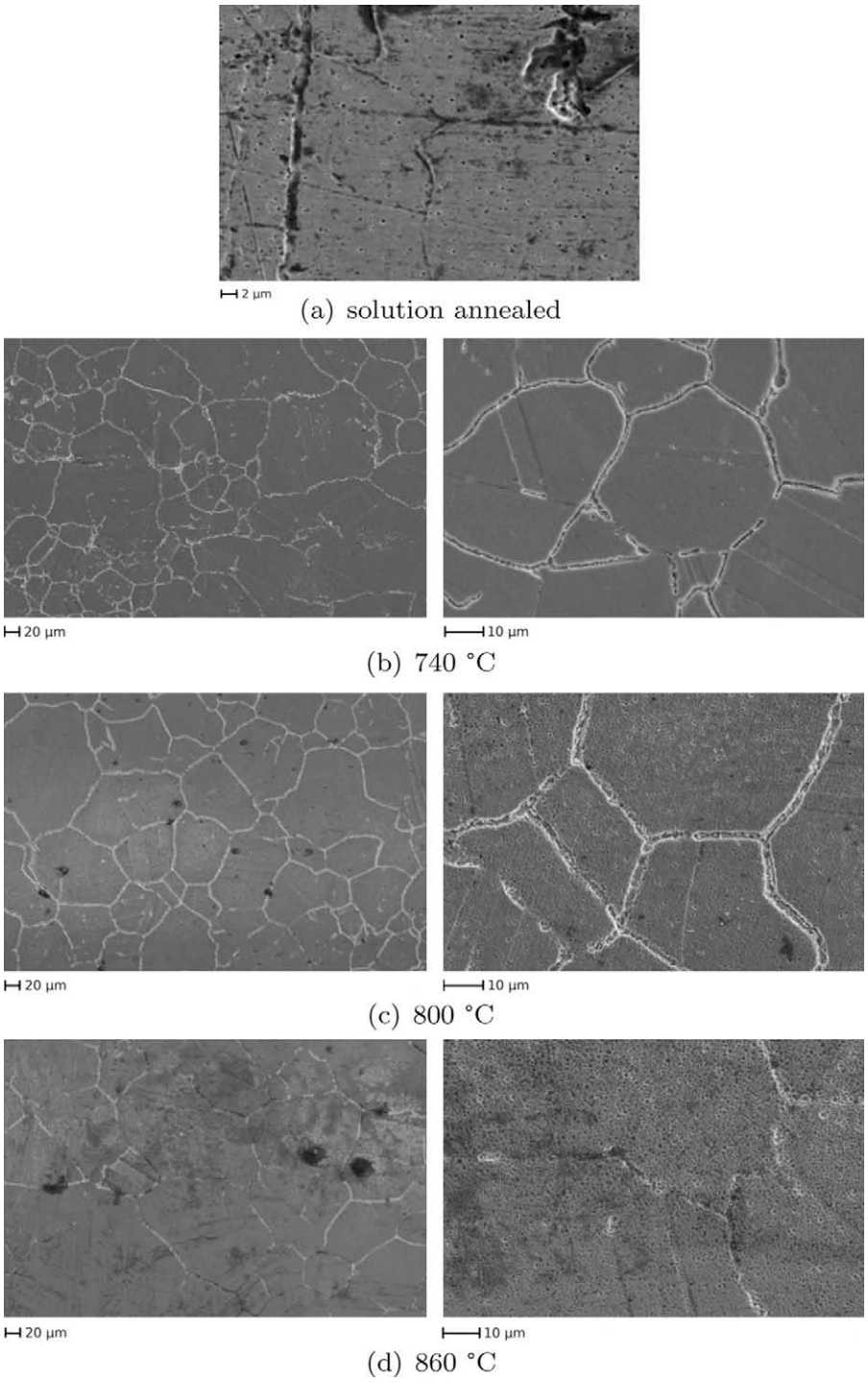

Fig. 10. Microstructural characterisation of EPR-test by means of SEM – solution annealed specimens + sensitization for 2 h at variable temperatures. (a) Solution annealed (b) 740 °C (c) 800 °C (d) 860 °C.

Please cite this article in press as: M. Prohaska et al., On the substitution of conventional corrosion tests by an electrochemical potentiokinetic reactivation test, Corros. Sci. (2010), doi:10.1016/j.corsci.2010.01.017

3.2.3. Stabilization annealed specimens + sensitization at 740 °C for various times

Depth of attack as well as dissolved volume increases slightly until a sensitization time of 10 h. After sensitization for 20 h the values of both surface parameters have noticeable high values (in conformity with Fig. 5).

3.3. Scanning electron microscopy (SEM) characterization

3.3.1. Solution annealed specimens + sensitization for 2 h at various temperatures

It is obvious, that the highest sensitization occurred between 740 and 800 °C. In the Streicher-test the attack around the grain

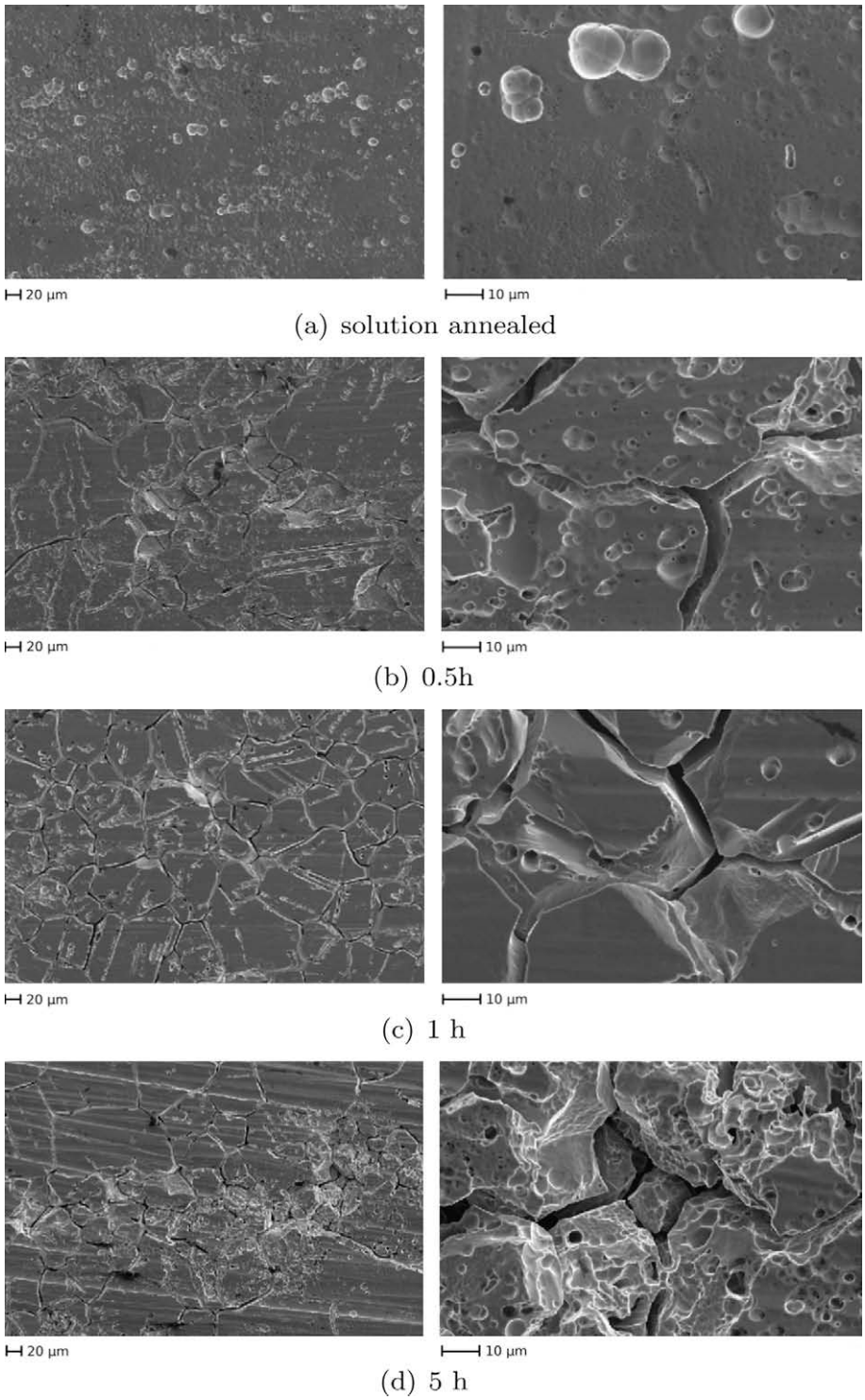

Fig. 11. Microstructural characterisation of Streicher-test by means of SEM – solution annealed specimens + sensitization at 800 °C for various times. (a) Solution annealed (b) 0.5 h (c) 1 h (d) 5 h.

Please cite this article in press as: M. Prohaska et al., On the substitution of conventional corrosion tests by an electrochemical potentiokinetic reactivation test, Corros. Sci. (2010), doi:10.1016/j.corsci.2010.01.017

boundaries appeared to be slightly deeper at 740 °C when compared to those in the sample given the 800 °C sensitization treatment. However, at 800 °C, it was evident that more grain dropping had occurred than was the case at 740 °C (this can be seen in Fig. 9b and 9c). Consequently, the higher corrosion rate seen in Fig. 3a for the 800 °C is attributed to more extensive grain dropping in this sample. This was verified by means of three-dimensional optical microscopy (Table 4).

The EPR method showed that the highest degree of sensitization was at 740 °C. The attack around the grain boundaries was deeper but less continuous than was seen for the 800 °C sensitization treatment (Fig. 10b and c). After sensitization at 860 °C the attack along grain boundaries was low. These observations were in conformity with the results shown in Fig. 3b.

3.3.2. Solution annealed specimens + sensitization at 800 °C for various times

Fig. 11 shows SEM-images of investigated Streicher-samples.

According to Fig. 4a, the intergranular attack increased with longer sensitization times in the Streicher-test. This could be

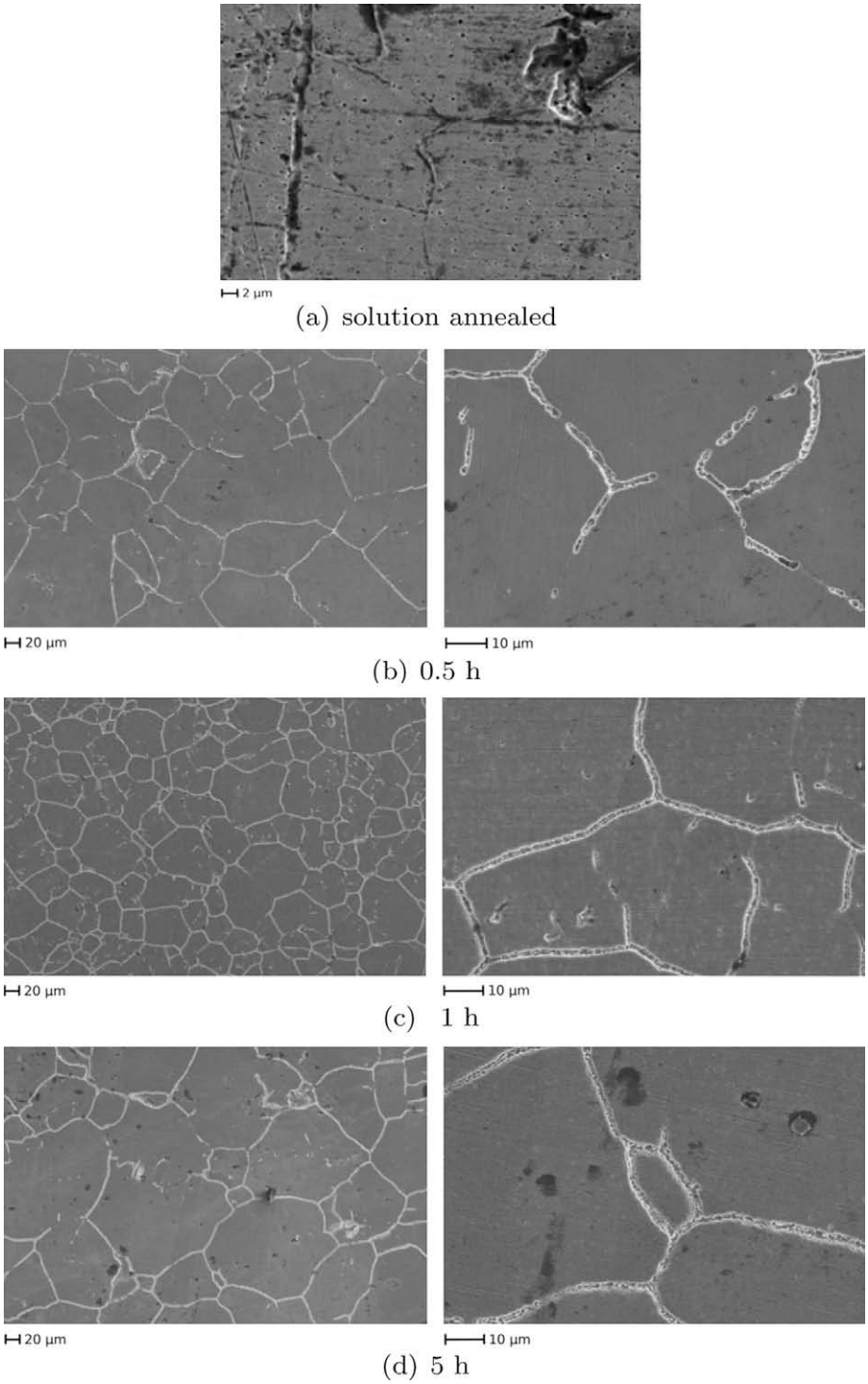

Fig. 12. Microstructural characterisation of EPR-test by means of SEM – solution annealed specimens + sensitization at 800 °C for various times. (a) Solution annealed (b) 0.5 h (c) 1 h (d) 5 h.

Please cite this article in press as: M. Prohaska et al., On the substitution of conventional corrosion tests by an electrochemical potentiokinetic reactivation test, Corros. Sci. (2010), doi:10.1016/j.corsci.2010.01.017

verified by the SEM-images shown in Fig. 11 and measurements with a three-dimensional light microscope (Table 4). After 5 h of sensitization a considerable number of grains dropped out and so the calculated corrosion rate was the highest.

Fig. 12 shows SEM-images of investigated EPR-samples. The corrosive attack adjacent to the grain boundaries was deepest after sensitization for only 0.5 h. The ditches appeared to be deep, however less continuous. After 1 h of annealing at 800 °C the ditches around the grains appeared to be more continuous and more shallow when compared to 0.5 h. Therefore, the Ir/Ia-ratio was lower compared to 0,5 h (Fig. 12c). Fig. 12d shows SEM-images of a specimen annealed for 5 h at 800 °C. The attack morphology was clearly shallowest and most continuous when compared to both 0.5 h and 1 h of annealing time.

3.3.3. Stabilization annealed specimens + sensitization at 740 °C for various times

Fig. 13 illustrates SEM-images of stabilization annealed specimens investigated in the Streicher-test.

The longer the sensitization time the higher is the corrosive attack (Fig. 13a, 13b and 13c). A considerable amount of grains dropped after 20 h of sensitization. As determined by means of Streicher-test and three-dimensional microscopy, susceptibility to intergranular corrosion increased with longer sensitization times.

This dependency was also examined by using the EPR-method. Fig. 14 shows images of stabilization annealed samples after various sensitization times. It is obvious, that intergranular attack occurred increasingly with time of sensitization. The morphology of the corrosive attack was increasingly localized at grain boundaries.

4. Discussion

During Streicher-test amount of corrosive attack is determined by quantity of dissolved volume of chromium depleted zones as well as by the amount of dropped grains. The higher the sensitization of the specimen the higher the amount of dropped grains and therefore, the extent of dissolved volume on the calculated corrosion rate decreases. When a continuous dissolution of grain boundaries occurs, corrosion rate during Streicher-test will peak because grain dropping is promoted. Contrarily, EPR-test is sensitive to the sensitized volume at, or connected to, the specimen's surface. Therefore, a deep and wide corrosive attack will lead to a high EPR-value. Continuity of the corrosive attack is not as striking as for the Streicher-test. Con-

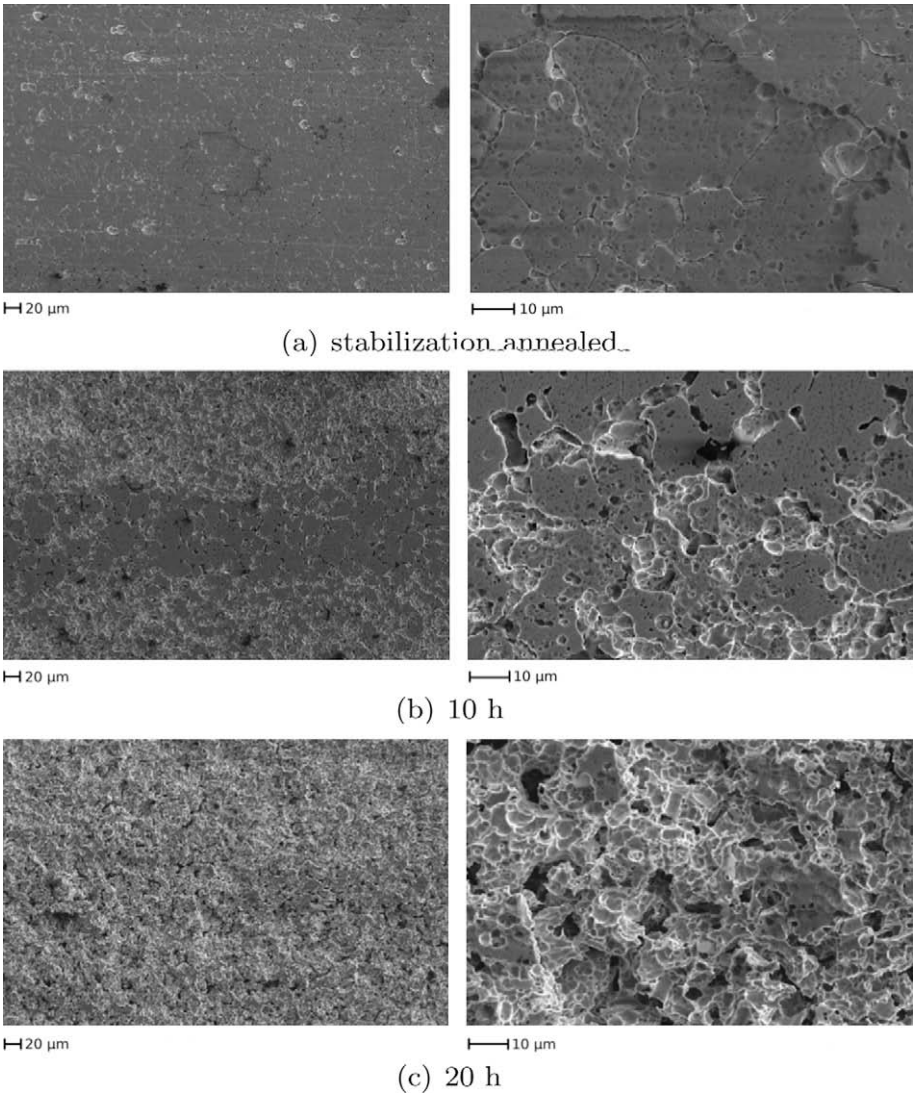

Fig. 13. Microstructural characterisation of Streicher-test by means of SEM – stabilization annealed + sensitization at 740 °. (a) stabilization annealed (b) 10 h (c) 20 h.

Please cite this article in press as: M. Prohaska et al., On the substitution of conventional corrosion tests by an electrochemical potentiokinetic reactivation test, Corros. Sci. (2010), doi:10.1016/j.corsci.2010.01.017

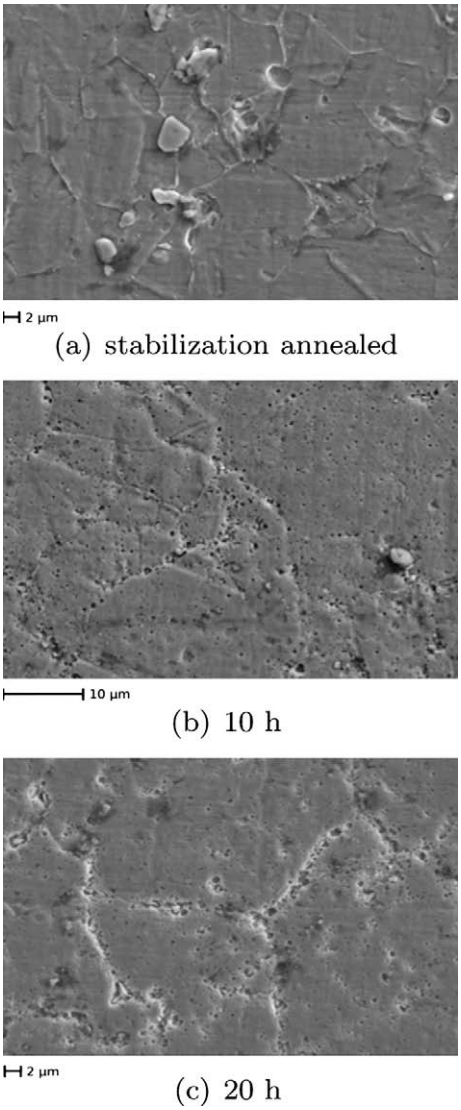

Fig. 14. Microstructural characterisation of EPR-test by means of SEM – stabilization annealed + sensitization at 740 °C. (a) Stabilization annealed (b) 10 h (c) 20 h.

sequently, the maximum of attack of EPR-test is shifted to lower temperatures and shorter sensitization times when compared to the Streicher-test.

In case of isochronic heat treatments, the ditches around the grains after Streicher-tests as well as after EPR-tests were deepest after sensitization at 740 °C when compared to 800 °C. SEM-investigations of the corrosive attack of EPR-tests revealed a higher continuity along grain boundaries after sensitization at 800 °C when compared to 740 °C. The difference of the maximum corrosion rate between EPR-(after sensitization at 740 °C) and Streicher-test (after sensitization at 800 °C) was obviously caused by a considerable amount of dropped out grains at 800°C (this can be seen in Fig. 9c) during Streicher-test. Contrarily, the deep, but however less continuous attack of grain boundaries of specimens sensitized at 740 °C (Fig. 10b) led to a high current density ratio during EPR-tests (high amount of dissolved volume), whereas grain dropping was not promoted.

In the isothermal series, the corrosion rate determined via Streicher-test increased, as expected, with longer sensitization treatments. The current density ratio examined by means of EPR-test exhibited a maximum after 0.5 h of sensitization and then declined.

Both effects, of sensitization time and temperature, could be explained by the relation between carbide precipitation and chromium diffusion from the bulk grain to the grain boundary. Several authors have found by examining concentration profiles with high-resolution techniques that after annealing at high temperatures and/or after longer times the degree of sensitization could be smaller due to chromium and/or molybdenum depletion from the bulk material to the grain boundaries [23,22,24]. Simultaneously, a higher number of secondary carbides occurred after sensitization at 800 °C when compared to 740 °C and after 5 h when compared to 0.5 h. This resulted in more continuous but less deep sensitized zones at higher temperatures and longer sensitization times. After 0.5 h of sensitization, secondary carbide precipitation (mainly M_6C) had just begun and therefore, the attacked chromium/molybdenum depleted zones in the surroundings of these carbides were deep but not continuous and so the evaluated current density ratio was rather high. The longer the sensitization treatment the more chromium/molybdenum from the adjacent grains could diffuse into the depleted zones and made them more shallow, although further M_6C precipitation took place. In consequence the Ir/Ia ratio declined. The influence of this process on the results of the Streicher-test was small compared to the increasing amount of dropped out grains after long sensitization treatments. The latter happened by further M_6C precipitation, which led to continuous dissolution of grain boundaries. So the corrosion rate determined by means of Streicher-test was continuously increasing, which was confirmed by three-dimensional optical microscopy.

The corrosion rate evaluated via Streicher-test for the stabilization annealed condition was rather small, but after 10 h of isothermal heat treatment at 740 °C it rose sharply. It was found that apart from the increasing susceptibility to intergranular corrosion the amount of dropped grains had strongly increased. The Ir/Ia ratio determined by means of EPR-test increased only slightly but almost constantly with increasing sensitization time.

Ir/Ia values are higher for stabilization annealed condition when compared to solution annealed specimens after sensitization times above 2 h as well as without sensitization treatment. The role of chromium/molybdenum diffusion in case of the solution annealed specimens has been already explained. In the solution annealed condition, there is only a small amount of primary NbC and negligible quantities of (Nb,Ti)C and M_6C in the matrix. Contrarily, in the stabilization annealed condition, the amount of primary NbC, (Nb,Ti)C and especially M_6C is considerably higher. Therefore, Ir/Ia values are higher in the stabilization annealed delivery condition compared to the solution annealed condition. Primary NbC causes a reduction of the effective carbon content in the matrix. Thus, further precipitation in the stabilization annealed condition during sensitization is impeded and the increase of Ir/Ia values with increasing sensitization times is low.

5. Conclusions

1. It is possible to replace the Streicher-test with the EPR-test, with some restrictions: First of all, it has to be assured, that the whole EPR-test procedure is carried out very accurately and precisely. The influence of the test procedure (especially avoidance of the formation of an overly thick passive film and selection of test parameters) is much stronger compared to the Streicher-test. Test parameters of EPR-test have to be selected in a way, that only a minor extent of uniform corrosion occurs during the test.

Please cite this article in press as: M. Prohaska et al., On the substitution of conventional corrosion tests by an electrochemical potentiokinetic reactivation test, Corros. Sci. (2010), doi:10.1016/j.corsci.2010.01.017

2. Mass loss evaluated by means of Streicher-test is strongly influenced by amount of dropped grains, whereas during EPR-test no grain dropping occurs. The current density ratio is directly related to the extent of dissolved specimen volume and thus, to the degree of sensitization (proportional to the size of chromium/molybdenum depleted zones).
3. Investigations on solution annealed specimens revealed that in this condition the EPR-test is more sensitive at shorter sensitization times. In contrast, in the stabilization annealed condition both tests show comparable results. These facts were related to the effects of carbide precipitation and chromium/molybdenum diffusion from bulk to grain boundaries at higher sensitization temperatures and longer sensitization times.
4. EPR-test is a promising investigation technique for detecting susceptibility to intergranular corrosion in nickel-based alloys, especially for research in laboratories (short testing time). However, specimen characterisation by means of optical and/or scanning electron microscopy is absolutely necessary after EPR-test to estimate the measured current density ratios and the type of attack. If applying this method in the field, the sensitive test procedure might be a problem to achieve reliable and reproducible results.

References

[1] Annual Book of ASTM Standards; Section 3: Metals Test Methods and AnaJytical Procedures, vol. 03.02, Wear and Erosion, Metal Corrosion, 2000.
[2] V. Čıhal, T. Shoji, V. Kain, Y. Watanabe, R. Stefec, Electrochemical Polarization Reactivation Technique: EPR – A Comprehensive Review, Fracture and Reliability Research Institute, Graduate School of Engineering, Tohoku University, 2004.
[3] V. Čıhal, Intergranular Corrosion of Steels and Alloys, Elsevier Science Publishers, BV, 1984. pp. 368.
[4] U. Mudali, R. Dayal, J. Gnanamoorthy, P. Rodriguez, Relationship between Pitting and Intergranular Corrosion of Nitrogen-bearing Austenitic Stainless Steels, ISIJ International 36 (1996) 799–806.
[5] A. Turnbull, P. Francis, M. Ryan, L. Orkney, A. Griffiths, B. Hawkins, A novel approach to characterizing the corrosion resistance of super duplex stainless steel welds, Corrosion 58 (2002) 1039–1048.
[6] R. Kilian, EPR Round Robin Test mit sensibilisierten austenitischen Stählen Teil 1: Auswertung der Ergebnisse nach dem JIS-Verfahren, Materials and Corrosion 52 (2001) 45–53.
[7] S. Schultze, J. Goellner, J. Panitz, EPR-Messungen in warmgehenden Anlagen, Materials and Corrosion 54 (2003) 958–965.
[8] P. Záhumenskỳ, S. Tuleja, J. Országová, J. Janovec, V. Siládiová, Corrosion resistance of 18Cr–12Ni–2.5Mo steel, annealed at 500–1050 °C, Corrosion Science 41 (1999) 1305–1322.
[9] V. Čıhal, R. Štefec, On the development of the electrochemical potentiokinetic method, Electrochimica Acta 46 (24-25) (2001) 3867–3877.
[10] S. Kumar, M. Banerjee, Improvement of intergranular corrosion resistance of type 316 stainless steel by laser surface melting, Surface Engineering 17 (2001) 483–489.
[11] U. Heubner, Nickel Alloys, CRC Press, 1998. pp. 309.
[12] R. Schimboek, G. Heigl, R. Grill, T. Reichel, J. Beissel, U. Wende, Clad pipes for the oil and gas industry – manufacturing and applications, Proceedings of Stainless Steel World United Pipelines (2004) 375–393.
[13] M. Sundararaman, P. Mukhopadhyay, S. Banerjee, Precipitation of the δ-Ni_3Nb phase in two nickel base superalloys, Metallurgical Transactions A 19A (3) (1988) 453–465.
[14] H.M. Tawancy, I.M. Allam, N.M. Abbas, Effect of Ni_3Nb precipitation on the corrosion resistance of Inconel alloy 625, Journal of Materials Science Letters 9 (1990) 343–347.
[15] M. Sundararaman, P. Mukhopadhyay, S. Banerjee, Carbide precipitation in nickel base superalloys 718 and 625 and their effect on mechanical properties, Superalloys 718, 625, 706 and Various Derivatives (1997) 367–378.
[16] L. Ferrer, B. Pieraggi, J. Uginet, Microstructural Evolution During Thermomechanical Processing of Alloy 625.
[17] M. Köhler, U. Heubner, The effect of final heat treatment and chemical composition on sensitization, strength and thermal stability of alloy 625, Superalloys 718, 625, 706 and Various Derivatives (1997) 795–803.
[18] V. Shankar, K. Bhanu Sankara Rao, S. Mannan, Microstructure and mechanical properties of Inconel 625 superalloy, Journal of Nuclear Materials 288 (2001) 222–232.
[19] C. Vernot-Loier, F. Cortial, J. Corrieu, Influence of heat treatments on corrosion behaviour of alloy 625, Forged Rod (1994) 795–806.
[20] M. Prohaska, T. Wernig, G. Mori, G. Tischler, R. Grill, Possibilities and limitations of replacing a conventional corrosion test with an electrochemical potentiokinetic reactivation method using the example of alloy 625, EuroCorr (Nizza, France, 06-10 September 2009), paper No. 7901, 1–13.
[21] Alicona Imaging GmbH – Area Analysis Automation Manual, IFM 2.2, Infinite Focus G3.
[22] Y.M. Pan, D.S. Dunn, G.A. Cragnolino, N. Sridhar, Grain-boundary chemistry and intergranular corrosion in alloy 825, Metallurgical and Materials Transactions A 31A (4) (2000) 1163–1173.
[23] H. Sahlaoui, H. Sidhom, J. Philibert, Prediction of chromium depleted-zone evolution during aging of Ni–Cr–Fe alloys, Acta Materialia 50 (2002) 1383–1392.
[24] H. Sahlaoui, K. Makhlouf, H. Sidhoma, J. Philibert, Effects of ageing conditions on the precipitates evolution, chromium depletion and intergranular corrosion susceptibility of AISI 316L: experimental and modeling results, Materials Science and Engineering A 372 (2004) 98–108.

Please cite this article in press as: M. Prohaska et al., On the substitution of conventional corrosion tests by an electrochemical potentiokinetic reactivation test, Corros. Sci. (2010), doi:10.1016/j.corsci.2010.01.017